Detection of Anomalous Structural Behaviour using Wavelet Analysis

[1]P. Moyo, [2]J.M.W. Brownjohn
School of Civil and Structural Engineering
Nanyang Technological University

[1] Research Student
[2] Associate Professor

Correspondence Address
Assoc. Prof. J.M.W. Brownjohn
Division of Structures and Mechanics
School of Civil and Structural Engineering
Nanyang Technological University
50 Nanyang Avenue
Singapore 639798
SINGAPORE

Tel +65-7904773
Fax +65-7910676

Email cjames@ntu.edu.sg

Abstract

Structural health monitoring (SHM) can be defined as the continuous monitoring of a bridge's state properties, such as static and dynamic response, in order to diagnose the onset of anomalous structural behaviour. This involves measuring and evaluating the state properties and relating these to defined performance parameters. The process of measuring state properties, either continuously or periodically, produces large quantities of data and by careful analysis of these data, sudden and gradual changes in the bridge's behaviour can be identified and characterised. The ability of wavelet transforms to detect abrupt changes, gradual change beginnings and ends of events make them well suited for the analysis of bridge health monitoring data. This paper presents the application of wavelet analysis to identify events and changes in structural state in a bridge during and after its construction.
Key words Wavelet analysis, wavelet transform, bridge health monitoring, structural health monitoring, change detection.

1 Introduction

A healthy transportation system helps to sustain industry and commerce of any country by ensuring public safety and societal well-being. Bridges constitute significant and critical discrete components of such a transportation system and they are among the most expensive investment asset of any country's civil infrastructure. They also have a long service life compared with most commercial products and are rarely replaceable once erected. Many countries have recognised the importance of maintaining the health of their bridge stocks and to this end numerous bridge authorities have introduced bridge management systems. Most current bridge management systems based on visual inspections in which visual inspection data are assigned condition states, which are then interpreted to assess the condition of the bridge and project its future behaviour. While inspection based bridge management systems provide a useful platform for developing bridge repair and maintenance programs and associated budgets, they also present some drawbacks. These include high manpower demands, inaccessibility of some critical areas of the bridge during inspections and lack of information on actual in-service loading environment. As a result some problems related to the structural performance of a bridge may go unnoticed until they become serious or expensive to repair. Shortcomings of inspection based bridge management systems, developments in signal processing tools, and availability of affordable instrumentation have motivated the development of instrumented monitoring systems. Numerous research efforts on instrumented bridge monitoring systems have been reported in technical papers, e.g. [1-6] to mention just a few. Most of these have focussed on developing methodologies for vibration based structural identification and damage detection. A detailed review of some structural identification and damage detection techniques is given in [7, 8]. In this paper attention is paid to analysis of long-term continuous monitoring of static performance data.

2 Structural Health Monitoring

Structural health monitoring (SHM) is defined here, in the context of a continuous long-term health monitoring system, as the continuous monitoring of a structure's response to the loading environment in order to diagnose the onset of anomalous structural behaviour. This involves continuous measurement of effects such as strains, stress, temperature, humidity, wind and accelerations, due to environmental loading, traffic loading, dead loads and material creep, and the analysis of these data to detect and characterise unusual structural behaviour. The goal of SHM is to complement existing infrastructure management strategies and thus SHM should be viewed as an integral part of an infrastructure management system, Fig. 1.

Typically a health monitoring system consist of a host computer, sensor excitation hardware, an integrated system of sensors, software and communication hardware. The host computer performs the task of controlling data acquisition and interpretation hardware in addition to storing recorded data in its hard disk, analysing the data, and communicating with remote computers. The sensor excitation and data interpretation hardware provides the link between the sensors and the host computer. This data acquisition hardware excites sensors and converts signals from sensors to appropriate engineering units such as strain, temperature, etc. Sensors are the nerves of the system, logging sensed data to the host computer

via the data acquisition system. Their selection for a particular system is governed by application, sensor sensitivity, power requirements, robustness and reliability. The software plays the important role of controlling the operating system, sensors, data analysis and communication. Data analysis involves reducing the data into useable information and presenting the data in meaningful formats for the user and the selected software should be user friendly and addressable from a remote site. Another important provision in the software is that it must be able to test and detect sensor fault and alert the operator. Communication capabilities form an important component of a health monitoring system; the user must be able to communicate with the host computer from a remote site as well as a portable computer hooked up to the system in the field. Possible communication links include, a modem and telephone line, a cellular connection, and telemetry or radio link.

SHM can therefore provide, online, the state of stresses, strains, temperature and even dynamic characteristics of a structure, an important but often missing ingredient in bridge management systems. In addition bridge engineers can use health-monitoring data to improve their understanding of the behaviour of new materials and structural systems, during and after construction. With the recent trends towards Build Own Operate and Transfer (BOOT) contracts, SHM can provide investors assurances about bridge behaviour during the ownership period and an up-to-date bridge condition at the end of the concession period.

Although potential advantages of SHM systems are attractive, some challenges need to be overcome before this technology can be fully exploited by bridge managers. This paper focuses on the problem of interpreting the meaning of measurements acquired by health monitoring systems. A brief overview a SHM system installed in the Singapore-Malaysia Second Link and a description the data interpretation problem are presented.

3 Monitoring Singapore-Malaysian Second Crossing

The Singapore-Malaysia Second Link (Fig. 2) is a pre-stressed box girder bridge carrying a dual carriageway with three lanes on each carriage. The bridge serves as a relief to the existing crossing located in northern Singapore. The bridge was completed in 1997 and opened to traffic in the same year. A SHM system was installed during construction in order to monitor the bridge's short-term and long-term behaviour and performance under construction loads, environmental loads, and vehicular loads. The SHM system includes a set of temperature sensors, stress cells, strain gauges and accelerometers distributed in three segments of the Singapore side of the bridge's main span. Details of the Second Link monitoring program are reported by Brownjohn and Moyo [9].

Experience gained with operating the SHM system in the Second Link shows that one of the main challenges in SHM is making sense of the large amounts of data acquired by networks of sensors. In particular strain data contain abrupt and short-lived changes that could be caused by potentially damaging actions for example ground motions, accidents or damage. In this study attention is paid to the analysis of hourly recordings of strain data made at one of the segments of the box girder

(Fig. 2), during and after construction. First some observations and comments about the strain data, leading to a definition of the interpretation problem are made.

(i) Positive strain change indicates compression while a decrease of strain signifies tension. Therefore a rapid drop in strain can be considered onerous for reinforced concrete structures, as this is likely to cause tension cracks.

(ii) All strain sensors installed in the bridge are synchronised. This implies that significant global changes in strain would be captured at the same time by the full set of sensors. In principle, by comparing strain readings of a set of sensors at a given location, one can identify both local and global changes in structural response.

(iii) Inherent in the strain response data is the uncertainty associated with random sampling, sensor faults and signal noise, making it difficult to characterise local effects.

(iv) Whereas considerable strain changes can easily be identified by visual inspection of data, isolating and locating intrinsic small strain changes (such as shown in Fig. 4-6) by visual inspection can be time consuming and inaccurate. For example by simple visual observation the top strain data (Fig. 3) can be divided into five distinct bands of activity associated with the construction of four segments of the bridge. However there are some specific strain events embedded within each band of data that are related to short-lived processes such as concreting, post-tensioning and shifting of form work traveller, which cannot be easily and accurately isolated from the data by visual inspection. A comprehensive health monitoring process should account for such changes as they may represent damaging effects to the structure. The identification and characterisation of these events constitutes the main theme of this paper.

The strategy adopted for identifying anomalous structural behaviour during the bridge's operation stage involves learning from data recorded at the construction stage. Known, identifiable events such as post-tensioning, concreting, shifting of form traveller are associated with possibly similar events that may occur during a bridge's service life such as ground movements, heavy traffic, wind gusts, settlement of supports, changes in the weather and relaxation of steel. Some of these changes, recorded during the construction of segments 27, 26, 25 and 24 are shown in Fig. 4-6. Changes arising from short-lived sudden events such as ground motions, heavy traffic, and wind gusts could be similar to post-tensioning effects while changes arising from short-lived gradual events such rainfall, support and relaxation of steel could be similar to casting events. Hence, by identifying such events during the bridge's service life one can make an intelligent guess about the cause. An approach for identifying the onset of hidden sudden changes and short-lived events from SHM data using wavelet analysis is proposed. Wavelet transforms have been chosen owing to their ability to detect abrupt changes and slowly varying changes. A brief background on wavelet analysis relevant for this work is given.

4 Wavelet Basics

Wavelets are wavy functions that are carefully constructed to have certain mathematical properties and derive the name from their oscillatory nature and decay properties. Wavelet properties relevant to the present work include, time-frequency

localisation, compact support, vanishing moments and smoothness. These properties ensure that fine-scale wavelet coefficients are only large where a function or its derivatives are discontinuous [10]. The basic idea of wavelet analysis is to represent general functions in terms of simpler fixed building blocks at different scales and positions. A theoretical treatment of wavelets and wavelet analysis may be found in [10,11].

4.1 Continuous Wavelet Transform

Using a selected analysing or mother wavelet function $\psi(t)$, the continuous wavelet transform of a function $Y_t \in L^2(R)$, is defined as;

$$W(a,b) = \int_{-\infty}^{\infty} Y_t \frac{1}{\sqrt{|a|}} \psi^* \left(\frac{t-b}{a} \right) dt \qquad (1)$$

where a and b are real constants and * denotes the complex conjugate. a is a scale or dilation variable and b represents time shift or translation The translation parameter, b, indicates the location of the moving wavelet window in the wavelet transform. Shifting the wavelet along the axis implies examining Y_t in the neighbourhood of the current window location. Thus, information in the time domain will remain, in contrast to Fourier transform where the frequency domain is used. The dilation parameter, a, indicates the width of the wavelet window. A smaller value of a implies a narrower wavelet window and a higher resolution.

4.2 Discrete Wavelet Transform

The wavelet transform can be discretised by selecting a dyadic subset of dilations and translations, i.e.

$$\psi_{j,k}(t) = 2^{-j/2} \psi(2^{-j} t - k) \qquad (2)$$

Associated with the discrete wavelet function is a scaling function given by,

$$\phi_{j,k}(t) = 2^{-j/2} \phi(2^{-j} t - k) \qquad (3)$$

The discrete wavelet transform of Y_t consists of wavelet coefficients, $d_{j,k}$ and scaling coefficients, $c_{J,k}$ given by;

$$d_{j,k} = \int_{-\infty}^{\infty} Y_t \, \psi^*_{j,k}(t) dt, \quad c_{J,k} = \int_{-\infty}^{\infty} Y_t \, \phi^*_{J,k}(t) dt, \text{ j=1,2,..J,} \qquad (4)$$
$$J = \log_2(n), \text{ n=number of samples}$$

Y_t can be reconstructed from these coefficients using

$$Y_t = c_{J,k} \phi_{J,k}(t) + \sum_{j=1}^{J} d_{j,k} \psi(t) = S_J + \sum_{j=1}^{J} D_{j,k} \qquad (5)$$

S_J is an approximation of Y_t at level $j=J$, and D_{jk} represents the difference between two successive approximations.

Wavelet coefficients are associated with changes in averages of Y_t on scale $s_j = n/2^{j-1}$ spaced at $\Delta t = n/2^j$ units apart. They are also nominally associated with frequency bands $\left[2^{-(s_j+1)}, 2^{-s_j}\right]$ [11], i.e. the wavelet function approximates a band pass filter with band pass $\left[2^{-(s_j+1)}, 2^{-s_j}\right]$. Due to the orthogonality of the DWT, wavelet coefficients and detail coefficients preserve energy and hence variance of the function Y_t leading to the result;

$$\left\|D_{jk}\right\|^2 = \left\|d_{j,k}\right\|^2, \quad \sigma_Y^2 = \tfrac{1}{N}\sum_{j=1}^{J}\left\|d_{jk}\right\|^2 = \tfrac{1}{N}\sum_{j=1}^{J}\left\|D_{jk}\right\|^2 \qquad (5)$$

Therefore the DWT decomposes a signal according to its frequency components, energy content, and variance composition in scales that can be viewed in the time domain. Note that since the contribution of wavelet coefficients and detail coefficients to the energy and variance of Y_t at a given scale is the same we can extract information about Y_t from either detail coefficients or wavelet coefficients without loss of accuracy.

Scaling coefficients , c_{Jk} , are associated with averages of Y_t on scale $s_J = n/2^{J-1}$ spaced at $\Delta t = n/2^J$ units apart.

In this study the we use the Daubechies family of wavelets denoted *D(N)* with order *2N* and support *2N-1*.

5 Application of Wavelet Analysis to SHM

5.1 Strain Model

Consider strain records, $Y_1, Y_2, \ldots, Y_n$, recorded at one hour intervals from a concrete structure over a long period. We can model the strains as a time series given by;

$$Y_t = C_t + T_t + R_t, \qquad t = 0,1,2,...,n, \qquad (6)$$

where,

C_t represents time dependent strains due to creep and shrinkage of concrete, which appear as a trend in the observed strain values. Fig. 7 shows a typical curve for creep in concrete. The curve suggests that creep effects can be modelled as a polynomial of degree $K \le 3$. Theoretically, creep in a concrete structure can be estimated using [12];

$$C_t = \varepsilon(t_o)[1+\varphi(t_o,t)] + \Delta\varepsilon[1+\chi\varphi(t_o,t)] + \varepsilon_{sh} \qquad (7)$$

$\varepsilon(t_o)$ =initial strain,

$\varphi(t_o,t)$ =time dependent creep coefficient

$\Delta\varepsilon$ =change in strain due to stress increment,

χ =aging coefficient

ε_{sh} =shrinkage strain

T_t represents strains induced by thermal dilation of concrete. This is largely due to diurnal and seasonal variations in temperature. Thermal strains induced by diurnal temperature changes oscillate with a period of about one day, while strains due to seasonal temperature variations would have a period typically greater than six months. The strain induced by thermal dilation of concrete is given by [13],

$$T_t = \alpha(A + T(t_s)) + \alpha T(t_d) \qquad (8)$$

α = coefficient of thermal expansion
A= average seasonal temperature
$T(t_s)$ = seasonal time-dependent temperature distribution of the structure
$T(t_d)$ = daily temperature distribution of the structure

R_t represents changes in strain due to random events. These events could include, transient events such as immediate settlement, change in weather, or abrupt changes such as, ground motions, accidents, short spells of weather changes, heavy traffic. We define transient events here as those incidents that occur continuously over a period less than 24hours, but greater than 4hours and abrupt events as those incidents that last less than 4hours. Our hypothesis is that these events would appear in Y_t as white noise, or uncorrelated data. The objective of this paper is to detect and estimate the locations of abrupt events from health monitoring data. We seek a time domain based approach which is fast, efficient and accounts for most influencing variables.

5.2 Wavelet Strain Model

The aim here is to decompose the strain time series Y_t into components associated with influencing variables and study each component to extract salient events. In particular we want to identify and locate potentially damaging events from those potions of Y_t related to random changes, R_t. Earlier it was noted that *D(N)* wavelets are approximate band pass filters with pass band $\left[2^{-(s_j+1)}, 2^{-s_j}\right]$, implying that each wavelet scale is associated with a range of frequencies. Also because a *D(N)* wavelet has *N* embedded differencing operations a trend of polynomial order $K \leq N$ can be reduced to zero in the wavelet coefficients. That is only the scaling coefficients or equivalently, approximations will contain the trend component.

Figure 8 shows time series plot temperature data recorded at segment 31, location A. Figure 9 shows the fast Fourier transforms (FFT) of the strain and temperature data. Energy is concentrated around 0.04 cycles per hour and 0.08 cycles per cycle corresponding to approximately 24 hours per cycle and 12 hours per cycle respectively, in both strain and temperature time series. Therefore the picks in the FFT plot of strain data occurring at 24 hour and 12 hour periods are largely due to daily temperature changes. We also note that the FFT for the strain signals is similar for 1997 and 1999 data. It is therefore proposed that under normal conditions the energy content and hence spectral density function of Y_t does not

change. A mapping of wavelet coefficients onto the strain FFT using the wavelet function band pass approximation shows that;

1. Wavelet coefficients d_{Jk} and $d_{(J-1)k}$ on scales s_J & s_J+1 are largely associated with the flat portion of the FFT, which corresponds to a random process. It is, therefore, proposed that wavelet coefficients d_{Jk} and $d_{(J-1)k}$ or equivalently, detail coefficients D_{Jk} and $D_{(J-1)k}$ are associated with changes occurring in the random component of Y_t, i.e. R_t in equation 6.
2. Wavelet coefficients $d_{(J-2)k}$ on scales s_J+2 are associated with 24 hour temperature variations while wavelet coefficients $d_{(J-3)k}$ on scales s_J+3 are related to 12 hour temperature variations. Looking at equation 6 these changes can be associated with T_t.

Hence by applying the DWT to hourly strain data we create a multi-level model in which each component of the influencing variables is associated with wavelet and scaling coefficients or equally, wavelet details and approximations as follows,

$$\mathrm{Y}_t \approx c_{J_c^l k}\phi_{J_c^l k}(t)+\left[A+\sum_{j=J_c^t}^{J_c^{t'}} d_{J_c^t}\psi_{J_c^t k}(t)\right]+\sum_{j=J-3}^{J-4} d_{jk}\psi_{jk}(t)+\sum_{j=J}^{J-1} d_{jk}\psi_{jk}(t) \qquad (9)$$

$$\mathrm{C}_t \equiv c_{J_c^l k}\phi_{J_c^l k}(t),\ T_t \equiv \left[A+\sum_{j=J_c^t}^{J_c^{t'}} d_{J_c^t}\psi_{J_c^t k}(t)\right]+\sum_{j=J-3}^{J-4} d_{jk}\psi_{jk}(t),\ \ R_t \equiv \sum_{j=J}^{J-1} d_{jk}\psi_{jk}(t)$$

$c_{J_c^l k}$ =scaling coefficients associated with creep due to sustained loading

$d_{J_c^t}$ wavelet coefficients associated with strains due to temperature variations.

It should be noted that long data records, typically greater than six months [13], are required to accurately model the long term effect of temperature on strain. The effect of creep and seasonal thermal is not the subject of this paper and will not be explored any further in this text.

In what follows attention is paid to R_t from which changes in strain related to random events can be identified. In particular detail coefficients are studied in order to extract strains associated with potentially damaging events.

5.3 Detection of Anomalous Structural Behaviour

Consider wavelet coefficients $\hat{d}_{jk}$ associated with random changes in Y_t. These coefficients consist of changes in average of Y_t and noise associated with random sampling.

$$\hat{d}_{jk} = d_{jk} + \xi_{jk} \qquad (10)$$

ξ_{jk} = white noise component with zero mean and variance σ^2.

We want to identify wavelet coefficients that represent random changes at low scales *j*, from the noisy coefficients. Assuming that under normal conditions strain Y_t vary smoothly with time, then abrupt changes would cause discontinuity in the variation of Y_t. Daubechies [11] showed that $\hat{d}_{jk}$ in the neighbourhood of the abrupt change is significantly higher than others. Therefore sudden changes in strain data can be detected by checking the magnitudes of wavelet coefficients against a critical value. A good initial value of this critical coefficient is a modified version of the universal noise threshold proposed by Donoho and Johnstone [14] given by [15];

$$\lambda = \sigma(\sqrt{4(\log n + \log\log n)}) \qquad (11)$$

In the proposed procedure wavelet coefficients are normalised to make it easy to compare them at different scales resolutions.

The level of noise in the measurements is usually unknown and should be estimated from the data. The approach used here is that proposed by Donoho and Johnstone [16], which uses wavelet coefficients at the highest level of resolution to estimate σ;

$$\sigma = \frac{median(\left| d_{J-1,k} - median(d_{J-1,k}) \right|)}{0.6745}, \text{ where } J = \log_2(n) \qquad (12)$$

To locate discontinuities we proceed as follows. Assume that random coefficients are located at β_i, $i=1,\ldots,q$, where q is a finite integer and q is unknown. The estimate $\hat{\beta}_1,\ldots,\hat{\beta}_q$ of $\beta_1,\ldots,\beta_q$ at each level *j* is constructed as follows.

1 Estimate λ

2 Find the first $|\hat{d}_{jk}|$ which exceeds λ identify its location , $\hat{\beta}_1$, over [0, n-1]

3 Find the second $|\hat{d}_{jk}|$ which exceeds λ and identify its location , $\hat{\beta}_2$, over $[0,n-1]\setminus \{\hat{\beta}_1 + t/2j : t \in \text{support}(\psi)\}$

4 Continue the procedure until the last $|\hat{d}_{jk}|$ that exceeds λ and estimate its location , $\hat{\beta}_q$, over $[0, n-1]\setminus \cup_{i=1}^{q-1} \{\hat{\beta}_i + t/2j : t \in \text{support}(\psi)\}$

5.4 Characterisation of Structural Response

Given two strain vectors ***x*** and ***y***, with continuous wavelet transforms $W^x(a,b)$ and $W^y(a,b)$, respectively, their wavelet power spectra are can be defined as [17];

$$WP^x(a,b) = \left| W^x(a,b) \right|^2 \qquad (13)$$

$$WP^{y}(a,b) = \left|W^{y}(a,b)\right|^{2} \tag{14}$$

The cross-wavelet power spectrum of the two vectors is given by;

$$WP^{xy}(a,b) = W^{x}(a,b)W^{y*}(a,b) \tag{15}$$

$W^{y*}(a,b)$ is the complex conjugate of $W^{y}(a,b)$

Wavelet power spectra give a time-scale distribution of energy in the strain signal and since the acquisition of strains is synchronised the energy content and distribution depicted by the cross-wavelet power spectrum shows the global strain variation in the bridge. At lower scales information about abrupt changes such as those caused by post-tensioning can be extracted, while higher scales give information about slowly varying, short-lived events similar to casting activities.

In order to make it easier to compare different wavelet power spectra, wavelet power spectra are normalised as follows;

$$NWP^{x}(a,b) = \frac{\left|W^{x}(a,b)\right|^{2}}{\mathrm{var}\{W(a,b)\}}, \tag{16}$$

$$NWP^{xy}(a,b) = \frac{W^{x}(a,b)W^{y*}(a,b)}{(\mathrm{var}\{W^{x}(a.b)\}\,\mathrm{var}\{W^{y}(a,b)\})^{1/2}} \tag{17}$$

6 Detection of Events During and After Construction of the Second Link

6.1 Monitoring During Construction

Fig. 3 shows strains recorded at segment 31 during the construction of four segments of the bridge and Table 1 lists times at which concreting, post-tensioning and shifting of form traveller were carried out for each segment. By visual inspection of the data it is not easy to identify the occurrence of these events. However a zoom into the data reveals abrupt changes and transient strain changes shown in Figs. 4-6. Our hypothesis is that if the bridge was subjected to forces of similar magnitude during its service life some form of damage may occur making identification of such patterns of change in strain data important. First we apply the model proposed in section 3 using *D(4)* wavelet and procedures described in section 4 to strain obtained during construction and then optimise the critical value λ. Equation 9 implies that we need only two scales of the DWT, $s_j=1$ and $s_j=2$, to extract information about random changes R_t from Y_t. A dyadic sample size, buffered on either side with a tail equal to the sample average was chosen to perform calculations by fast algorithms of Mallat [18]. The purpose of the buffer, which is removed after decomposition, is to minimise edge effects introduced by the wavelet transform algorithm.

By comparing the location of coefficients larger than the critical value to the construction program in Table 1, we note that the DWT identifies the occurrence of all known events associated with the construction of segments 27, 26, 25 and 24 (Fig. 10), including some unknown events. A closer look at the data shows that these unknown events are indeed related to significant sudden changes in the strains, see for example Fig. 11 showing strain change related to event located at t=400. The most prominent coefficients are those associated with post tensioning activities. Considering such events as severe a second threshold can be defined, at this level, to isolate these severe responses. This second threshold level was empirically found (using coefficients associated with post tensioning events) to be approximately 2.0λ. Since the recording of strain data is synchronous a measure of dissociation between two strain data gives information about localised changes. Dissociation between two data sets is commonly measured using a semivariogram [17]. Following the definition of a semivariogram, [19], a wavelet semivariogram can be defined as;

$$WSV^{XY} = \frac{1}{2}\left|D_{jk}^{X} - D_{jk}^{Y}\right|^2 \qquad (18)$$

The wavelet semivariogram (Fig. 12) for strains recorded during construction shows four distinct peaks corresponding to post-tensioning of segments 27, 26 25 and 24 indicating that although post-tensioning affects the global behaviour of the bridge, the event has some degree of localisation.

Fig. 13 shows the normalised wavelet power spectrum for the top strains at segment 31. The spectrum shows that most of the power is concentrated within the scales 6-36, while scales 36-84 are characterised by isolated concentrations of power. Above scale 84 the wavelet spectra divides the power into five distinct periods of activity. The cross wavelet power spectrum for the strains (Fig. 14), show little difference from the wavelet power spectra of the time series indicating the close similarity between the two time series. A three dimensional view of the cross wavelet power spectra (Fig. 15) reveals high peaks at lower scales, which are associated with abrupt changes in strains. The concentration of power within the scale 6-36 can be related to daily temperature cycles, while power concentrations at scales 36-84 represent the occurrence of short-lived changes, such as concreting and the five bands of high power above scale 84 depict ends of segment construction. In contrast to the wavelet semivariogram, the cross wavelet power spectrum gives a measure of association between two strain data, enabling global structural response to be characterised.

6.1 Monitoring After Construction

One abrupt strain change was identified by the DWT from the selected data (Fig.16). The change is a loss of tension and is similar to strain change resulting from post-tensioning.

The wavelet semivariogram (Fig. 17) does not show any strong dissociation between strain data indicating that there were no significant localised changes during this period.

The cross wavelet power (Fig. 18) indicates little activity from time *t=0* to time *t=400* hours, after which strain data is characterised by a series of activities accompanied by short-lived strain fluctuations. Fig. 19 shows the transitory strain change occurring at time *t=650* to *t=690*.

7 Conclusions

Strain data from a long term SHM system has been expressed as a multi-scale model in which each wavelet scale or set of scales is associated with variables influencing strain change. This representation allows the variables to be monitored individually. The paper demonstrates the use of wavelet analysis to detect the onset of anomalous behaviour by monitoring random events occurring on a bridge. However the proposed procedure does not give information on the effect of these anomalous events on structural behaviour, that is, 'did the structure experience some damage after the event?' In as health monitoring system such information is useful to minimise false alarms. False alarms could arise for example if a heavy truck crosses the bridge during recording, or if there is a sudden change in the weather, such as rainfall. Further investigations are on going on these subjects.

6 References

1. J.D. Achenbach, B. Moran, A. Zulfiqar 1997 Proceedings of the International Workshop on Structural Health Monitoring, 179-190. Techniques and Instrumentation for Structural Diagnostics.
2. A.E. Aktan, A.J. Helmicki, V.J. Hunt 1996 Proceedings of Building an International Community of Structural Engineers Congress 2, 750-757. Issues Related to Intelligent Bridge Monitoring.
3. S. Alampalli and G. Fu 1994 Transportation Research Record 1432, 59-67. Instrumentation for Remote and Continuous Monitoring of Structure Conditions.
4. J.R. Casas and A.C. Aparicio1998 Journal of Experimental Mechanics 38, 24-28. Monitoring of the Alamillo Cable-stayed Bridge During Construction.
5. M.S. Cheung 1997 Proceedings of the Seventh International Offshore and Polar Conference 2, 10-16. Instrumentation and Research Program on Confederation Bridge.
6. H.S. Kwong, C.K. Lau, K.Y. Wong 1995 Restructuring America and Beyond Structures Congress-Proceedings, American Society of Civil Engineers, New York, USA, 264-267. Monitoring System for Tsing Ma Bridge.
7. S.W. Doebling, C.R. Farrar, M.B. Prime, D.W. Shevitz 1996 Los Alamos National Laboratory Report LA 13070-MS. Damage Identification and Health Monitoring of Structural and Mechanical Systems From Changes in their Vibration Characteristics: A Literature Review.
8. S.W. Doebling, C.R. Farrar 1999 American Society of Civil Engineers Committee on Structural Identification of Constructed Facilities. The State of the Art in Structural Identification of Constructed Facilities.

9. J.M.W. Brownjohn and P. Moyo 2000 2nd International Conference on Experimental Mechanics, 29/11-1/12 2000. Monitoring of Malaysia-Singapore Second Link During Construction.
10. C.K. Chui 1992 Introduction to Wavelets, p264. Academic Press, San Diego.
11. I. Daubechies 1992 Ten Lectures on Wavelets, p 357. Society for Industrial and Applied Mathematics, Philadelphia.
12. A. Ghali and R. Favre 1994 Concrete Structures: Stresses and Deformations, p 464 E & FN Spon, Chapman and Hall, London.
13. Z. Smerda and V. Kristek 1988 Creep and Shrinkage of Concrete Elements and Structures, p 296. Elsevier Science Publishing Company, New York.
14. D.L. Donoho and I.M. Johnstone 1994 Biometrica 81, 425-455. Ideal Spatial Adaption by Wavelet Shrinkage.
15. F. Abramovich and A. Samarov 2000 Department of Statistics and Operations Research, Tel Aviv University, Technical Report RP-SOR-00-02. On one-sided estimation of a sharp cusp using wavelets.
16. D.L. Donoho and I.M. Johnstone 1995 Journal of American Statisticians Association 90, 1200-1124. Adapting to unknown smoothness via wavelet shrinkage",
17. C. Torrence and G.P. Compo 1998 Bulletin of the American Meteorological Society 79, 61-78. A Practical Guide to Wavelet Analysis.
18. S. G. Mallat, S. G. 1989 IEEE Transactions on Pattern Analysis and Machine Intelligence 11, 674-693. A Theory for multi-resolution signal decomposition: the wavelet representation.
19. B. Bacchi and N.T. Kottegoda 1995 Journal of Hydrology 165, 311-348. Identification and Calibration of Spatial Correlation Patterns of Rainfall.

Table 1: Construction Program : Time (Hours from 29-04-1997 00:00:00hrs)

Activity	Segment			
	27	26	25	24
Concreting	91-95	280-288	496-500	700-710
Post-Tensioning	155-156	328-329	538-540	778-779
Shifting form traveller	180-182	352-355	553-558	950-954

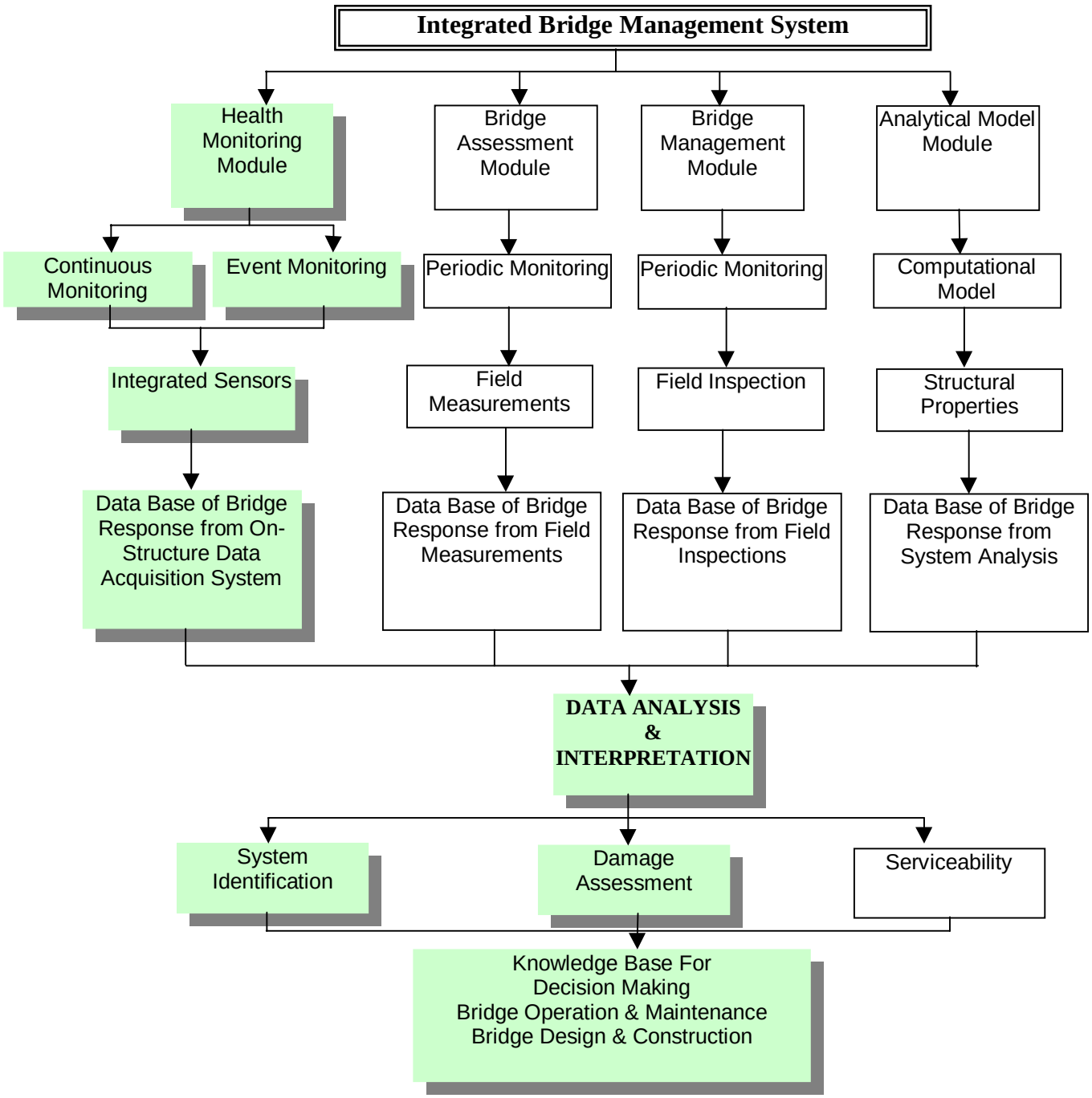

Fig. 1 : An Integrated Bridge Management System

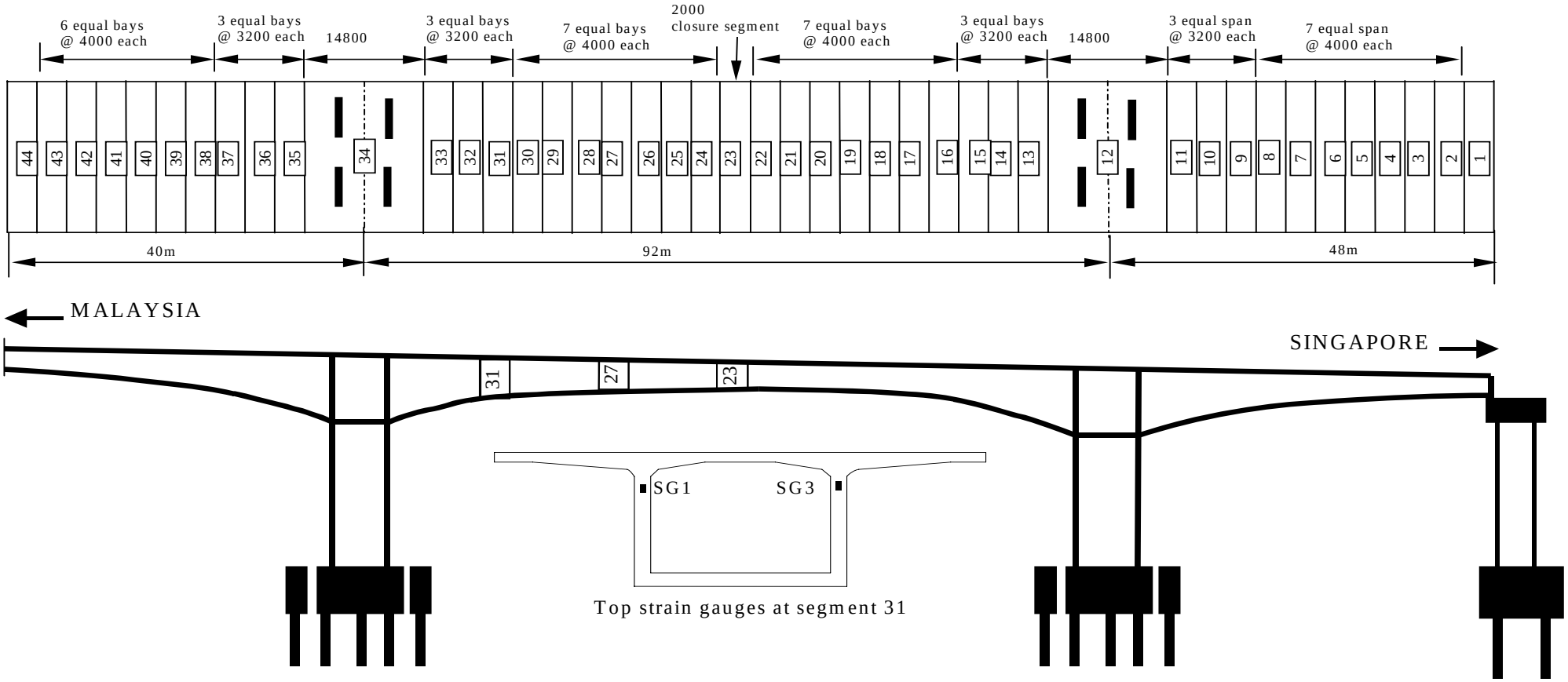

Fig. 2 : Bridge Layout

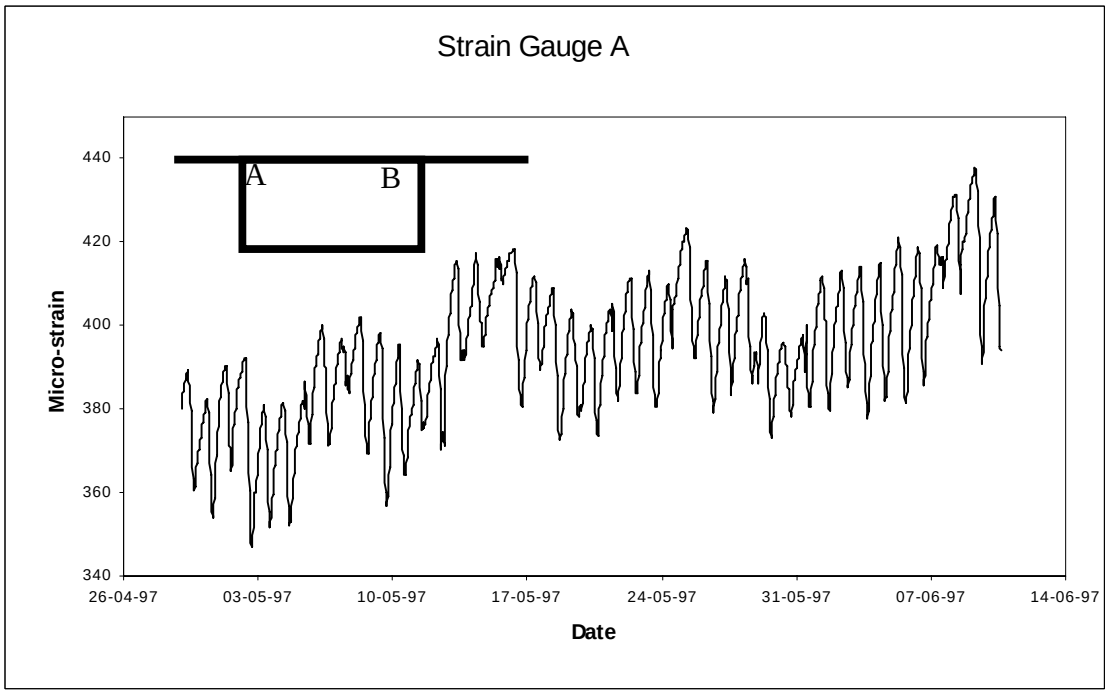

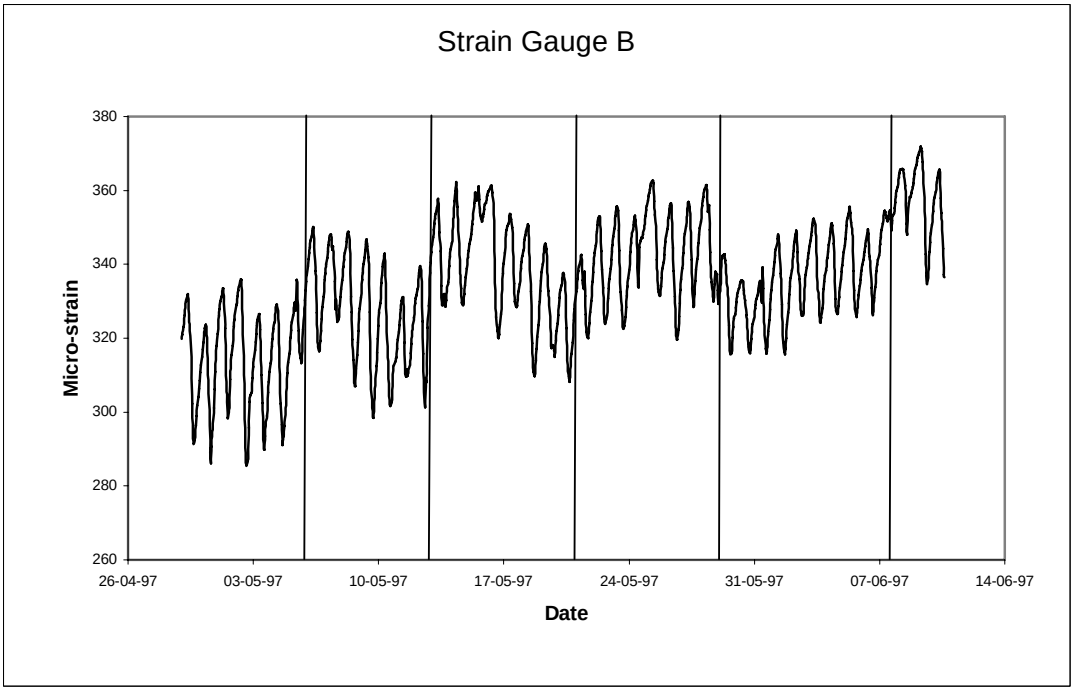

Fig. 3a: Strain Data recorded during

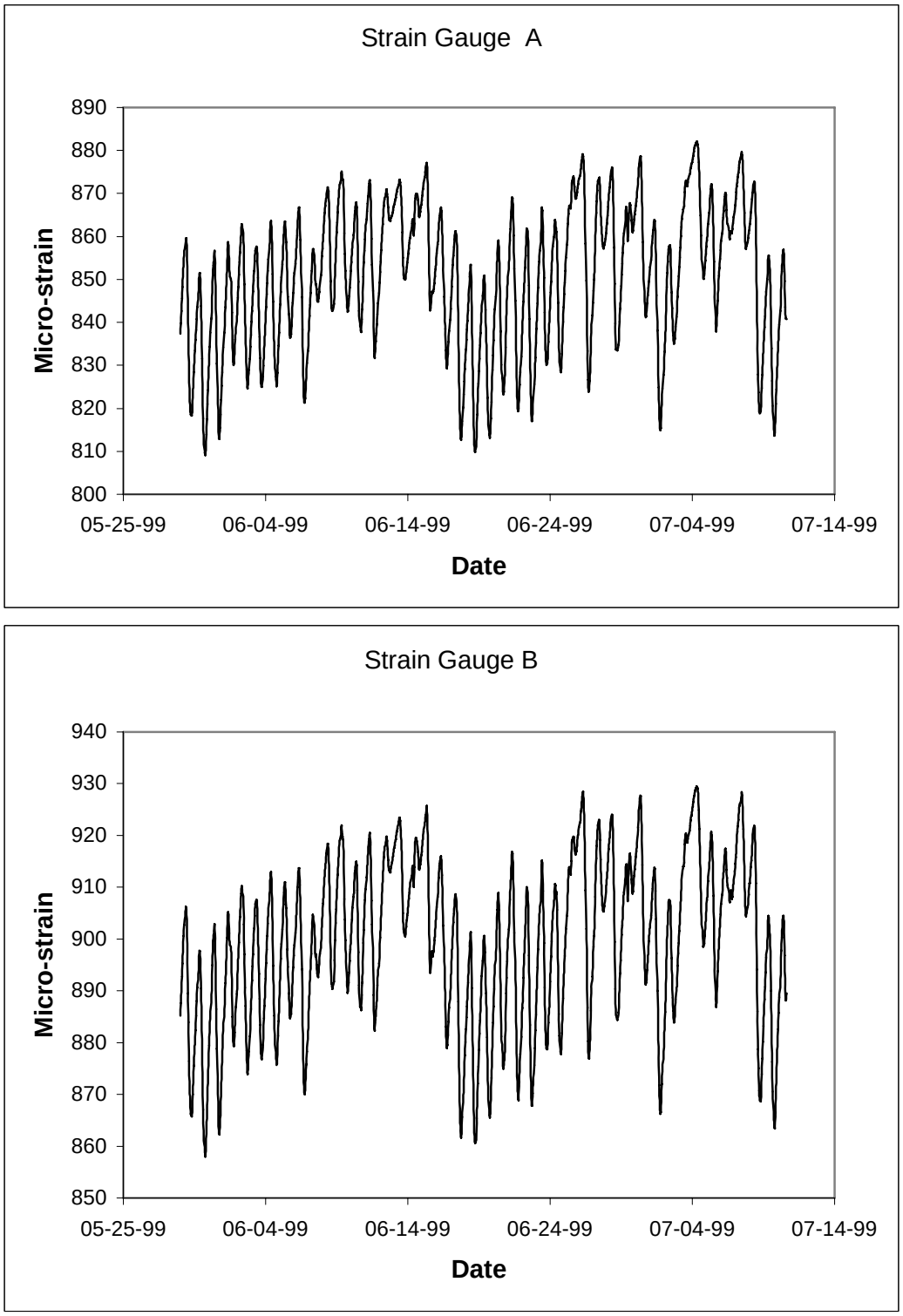

Fig. 3b: Strain data recorded after construction

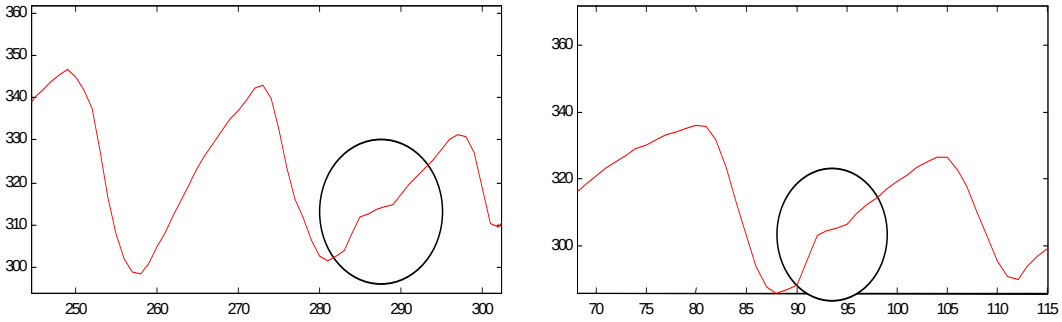

Fig. 4 Concreting events

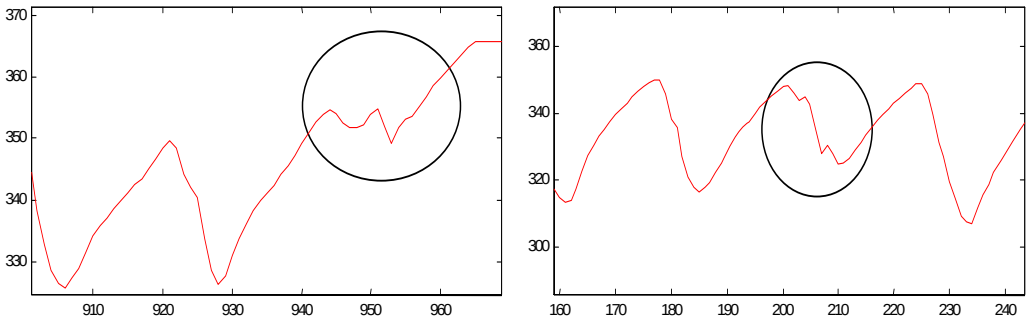

Fig. 5 Shifting Events

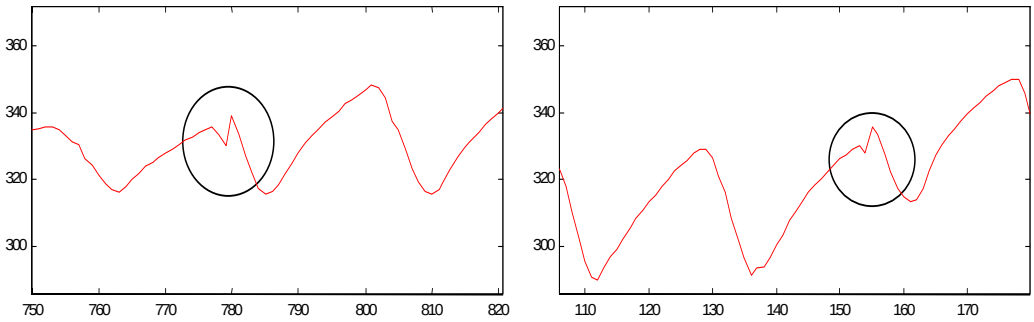

Fig. 6 Post-Tensioning Events

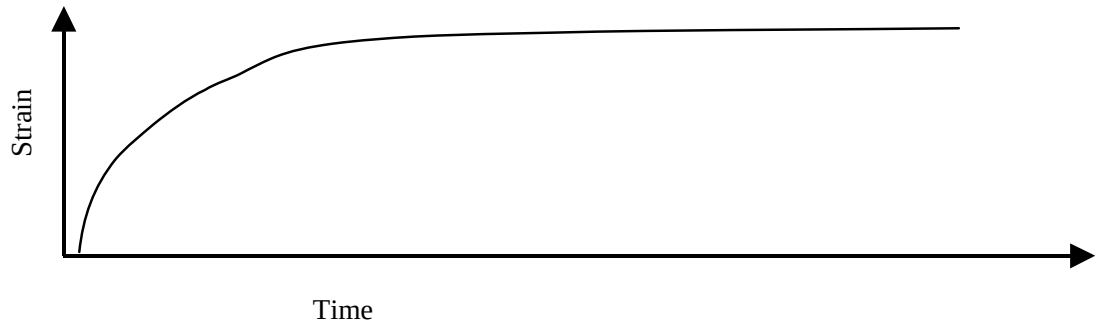

Fig. 7: Typical Strain-Time Curve

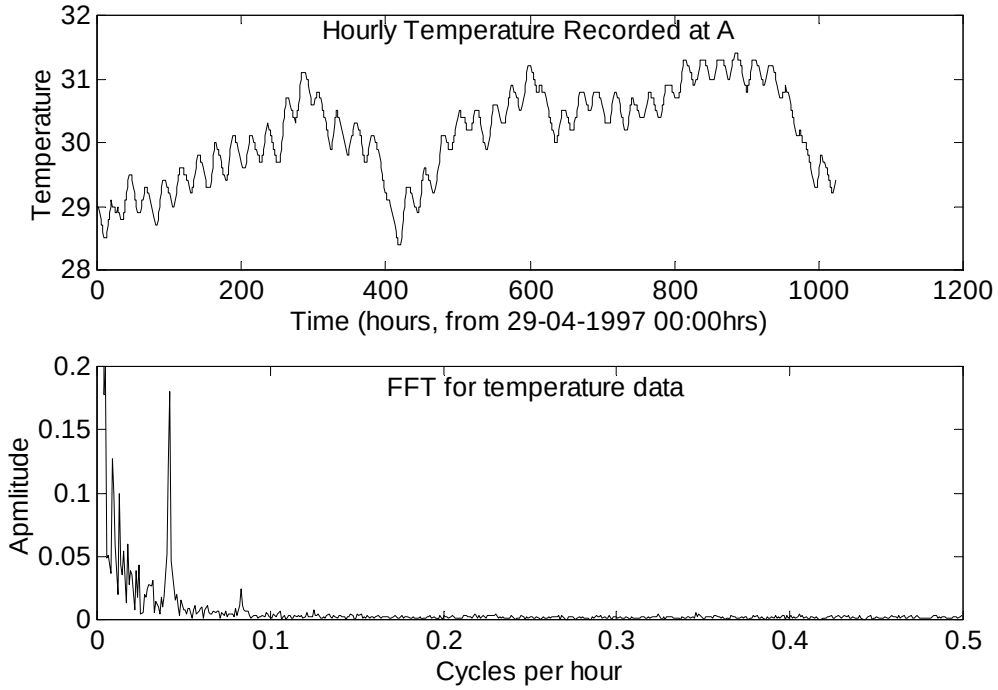

Fig. 8: Fourier Transform of Temperature Data

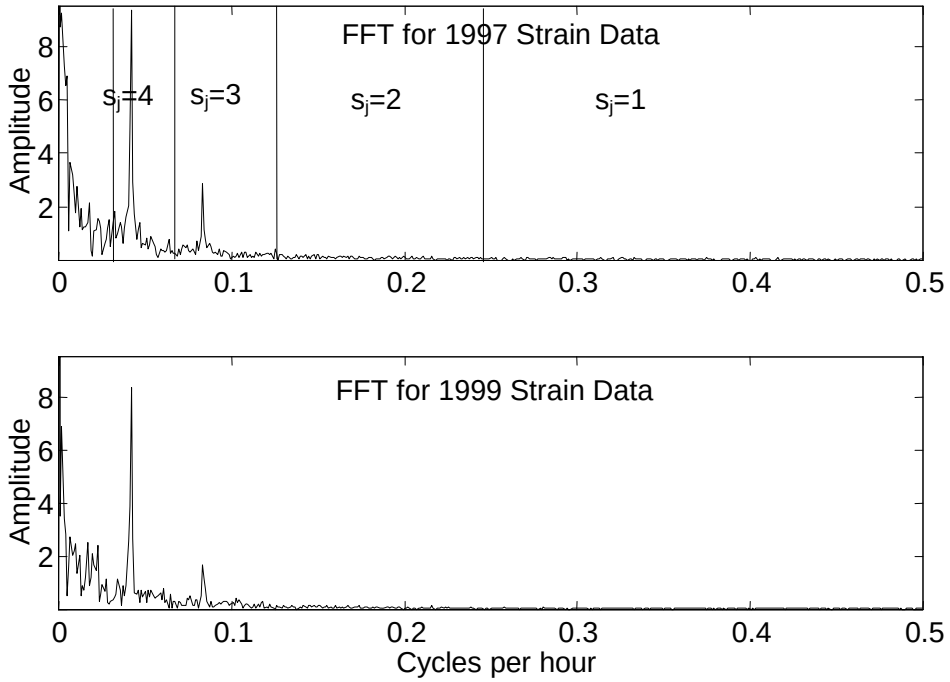

Fig. 9: Fourier Transform of Strain Data

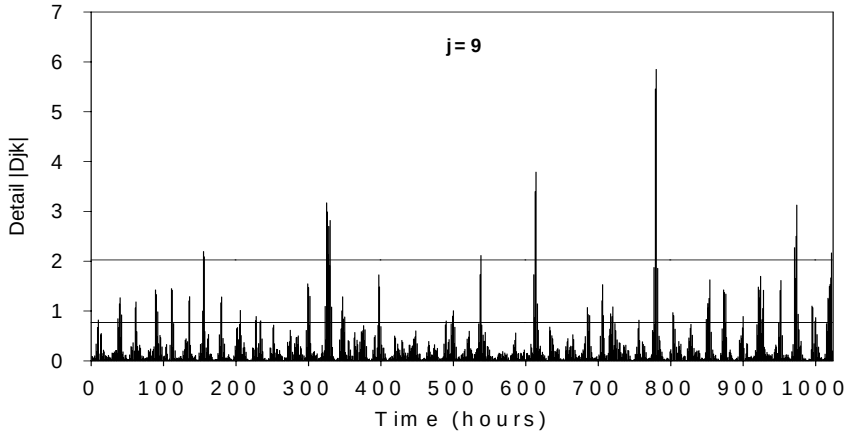

Fig. 10: Event identification using wavelet detail coefficients.

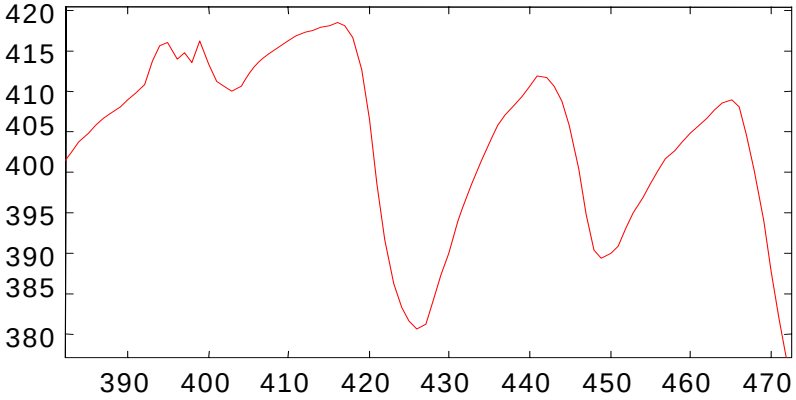

Fig. 11: Identified unknown event.

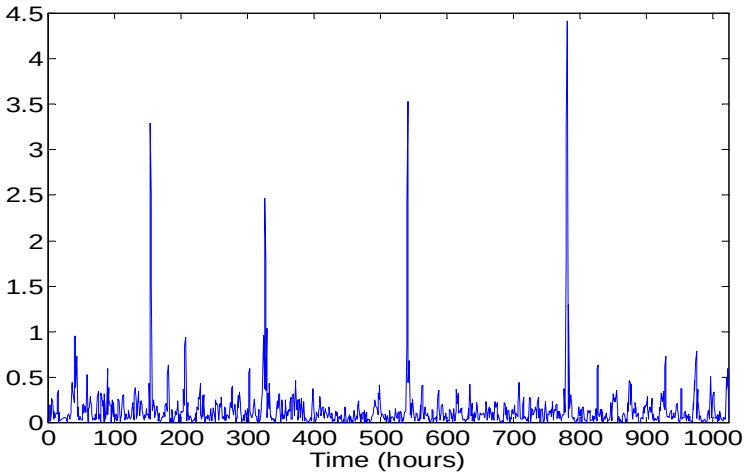

Fig. 12: Wavelet semivariogram for data recorded during construction.

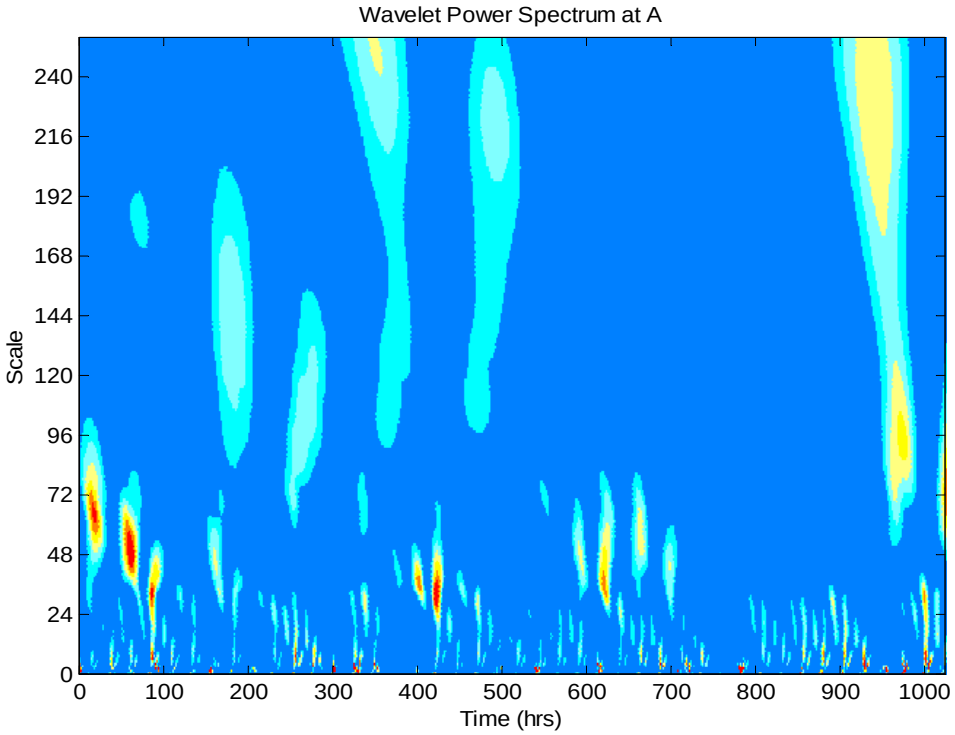

Fig. 13: Wavelet Power Spectrum for Strains at A

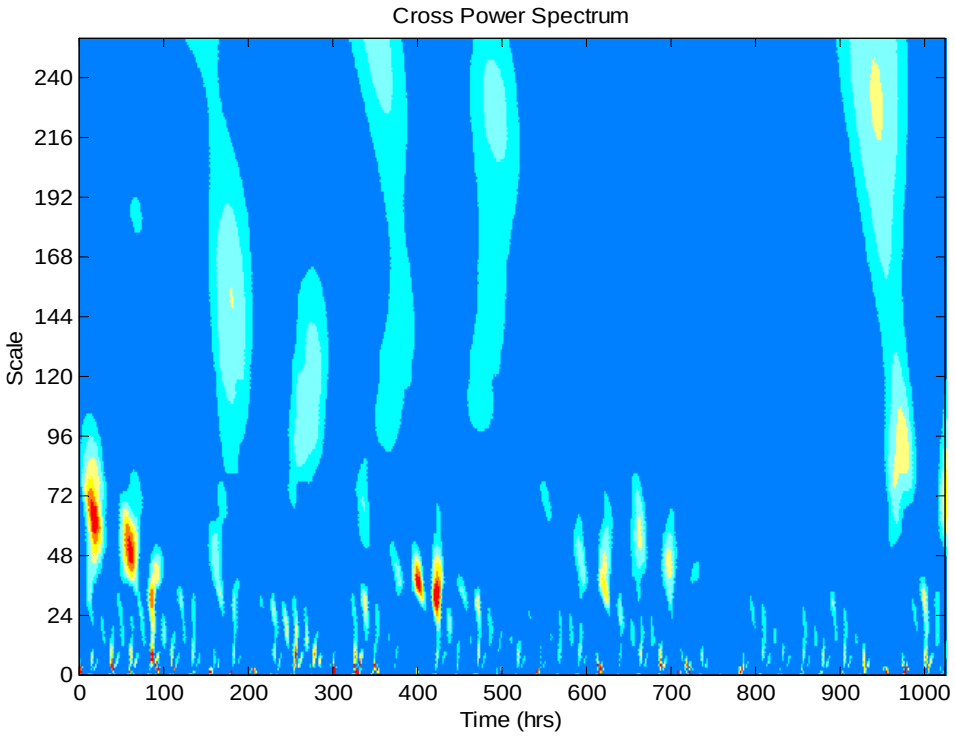

Fig. 14: Cross Wavelet Power Spectrum for strains at A and B

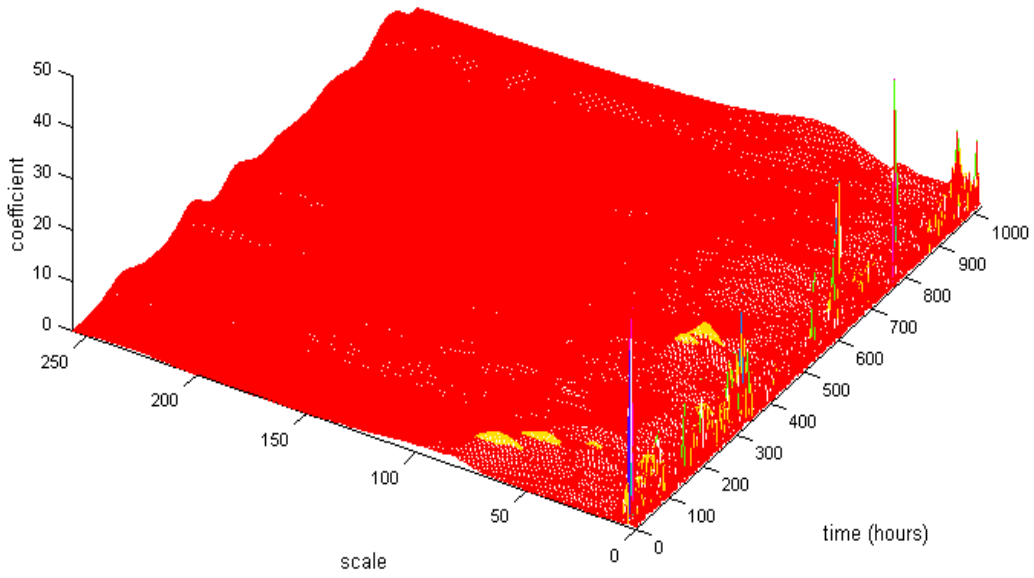

Fig. 15: Cross wavelet spectrum for strains at A and B

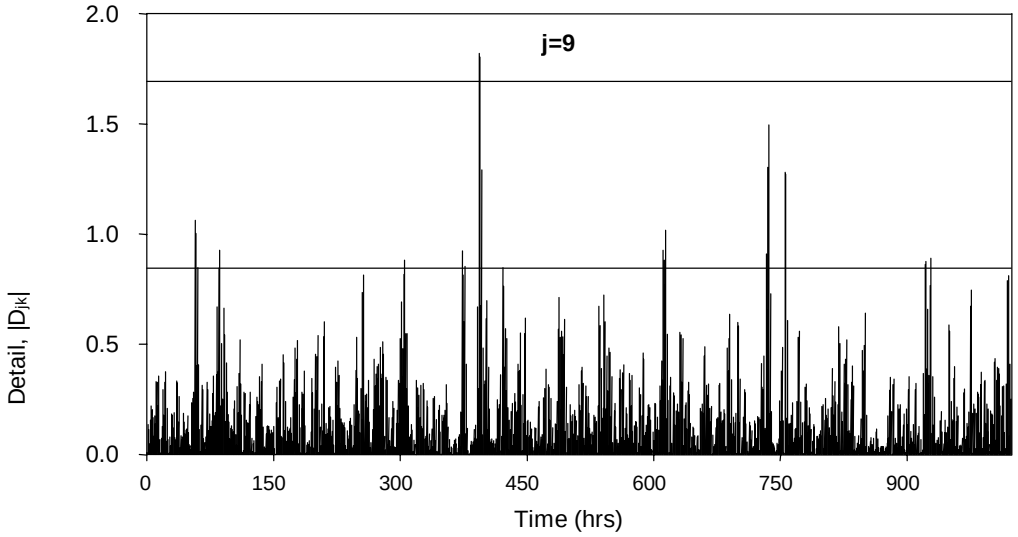

Fig. 16: DWT Decomposition After Construction

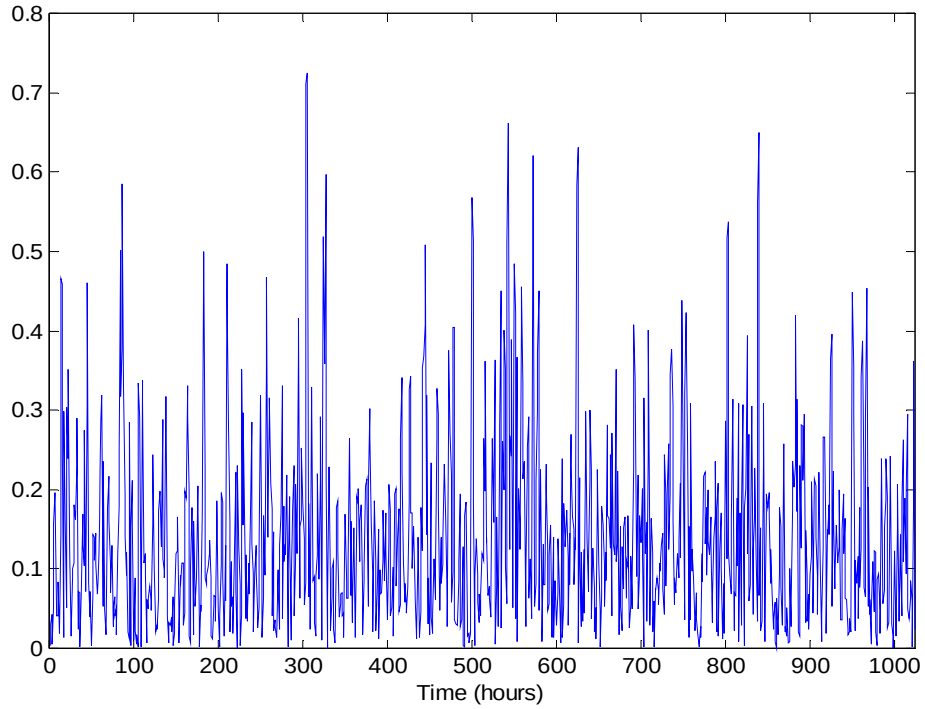

Fig. 17: Wavelet Semivariogram

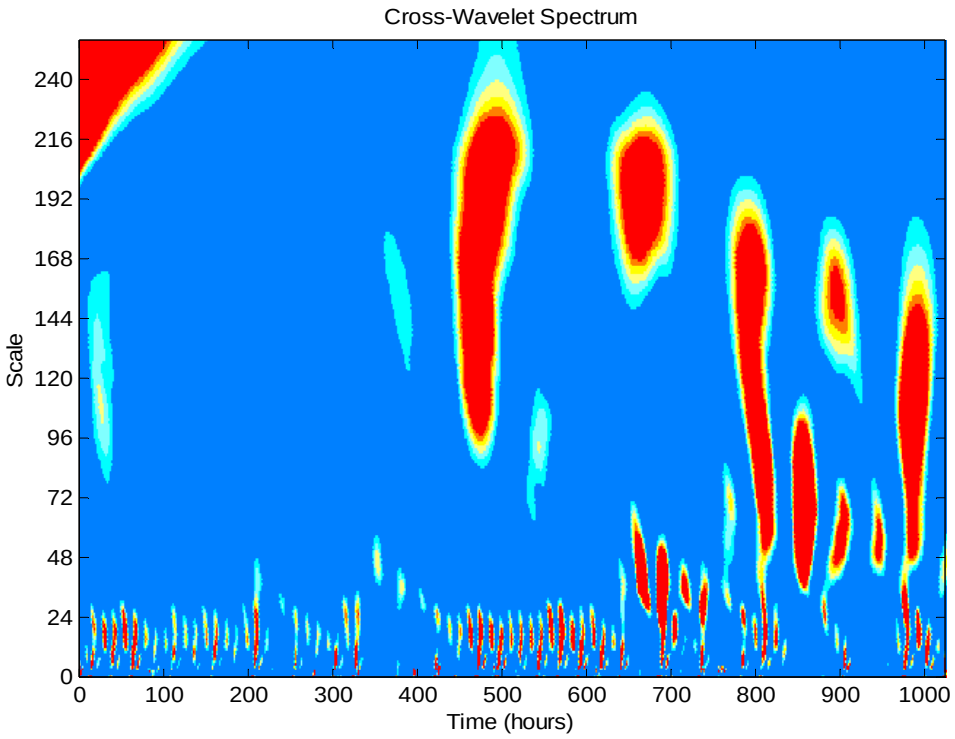

Fig. 18: Cross-Wavelet Spectrum

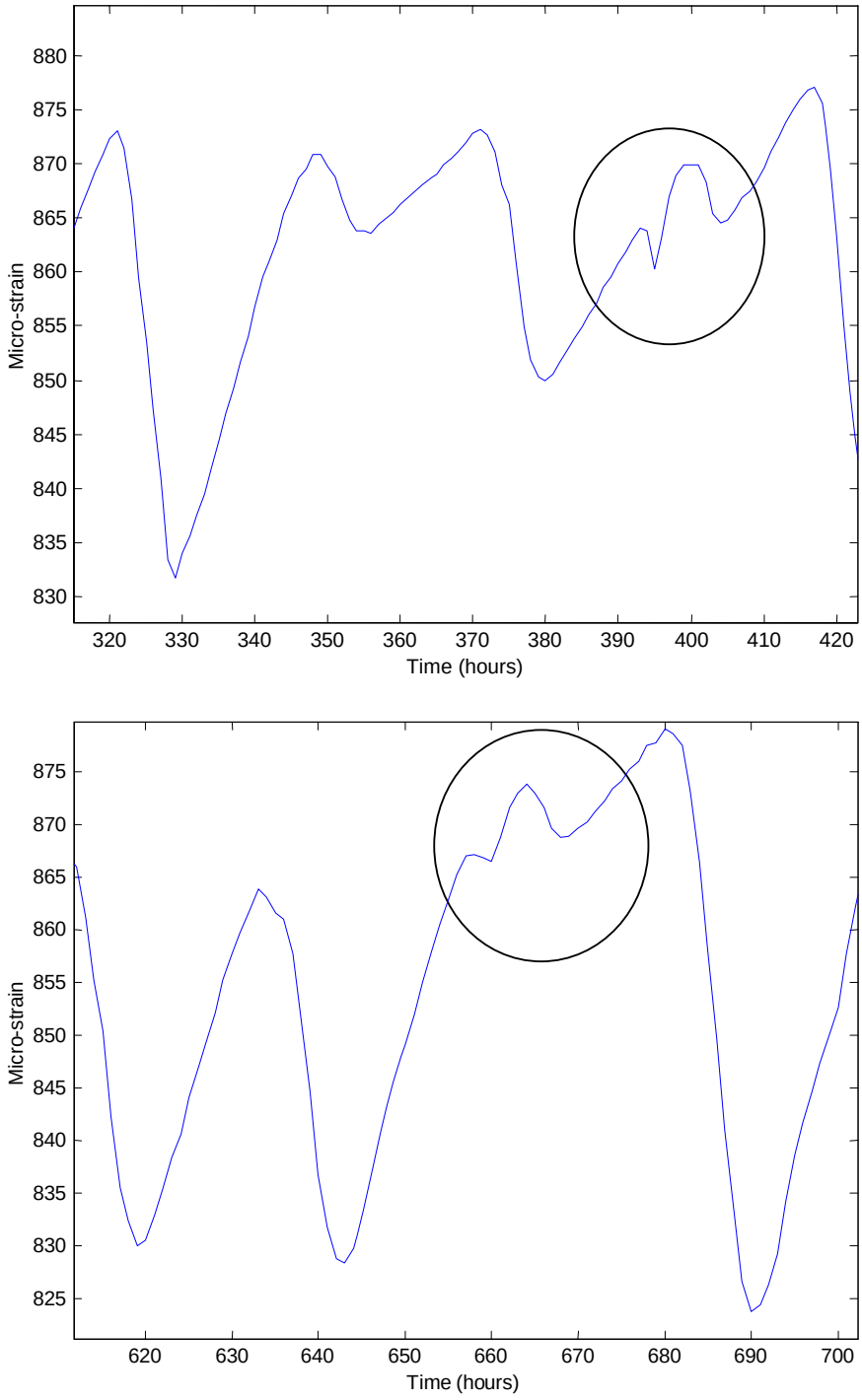

Fig. 19: Some events identified from post construction strain data.